675

Asymmetry Measurements for Dimuon Production In the J/ψ Mass Region

by

R. Ditzler, D. Hill, H. Spinka, R. Stanek, K. Toshioka,
D. Underwood, R. Wagner and A. Yokosawa
Argonne National Laboratory, Argonne, Illinois

Y. Hemmi, K. Imai, R. Kikuchi, K. Miyake, T. Nakamura,
K. Nishimura and N. Tamura
Kyoto University, Kyoto, Japan

H. Azaïez, K. Kuroda, A. Michalowicz, D. Perret-Gallix
LAPP, Annecy, France

G. Shapiro
Lawrence Berkeley Laboratory
University of California, Berkeley, California

D. H. Miller and C. LeRoy
Northwestern University, Evanston, Illinois

M. Corcoran, H. E. Miettinen, T. A. Mulera, G. S. Mutchler,
G. C. Phillips and J. B. Roberts
Rice University, Houston, Texas

R. Birsa, F. Bradamante, S. Dalla Torre-Colautti, M. Giorgi, L. Lanceri
A. Martin, P. Moras, A. Penzo, P. Schiavon and A. Villari
INFN, Sezione di Trieste, Trieste, Italy

January 29, 1981

Overseas Spokesman:
K. Miyake
Kyoto, University
Kyoto, Japan

U.S. Spokesman:
A. Yokosawa
Argonne National Laboratory
FTS: 972-6311
Commercial: (312) 972-6311

Table of Contents

Page

I. INTRODUCTION 3

II. PHYSICS JUSTIFICATION 3

III. EXPERIMENTAL SETUP 6

IV. POLARIZED BEAM 8

V. POLARIZED TARGET 9

VI. TRIGGER REQUIREMENTS AND DATA COLLECTION 9

VII. EXOECTED BACKGROUND 10

VIII. RATES AND RUN PLAN 10

IX. APPARATUS 11

References 13

Figure Captions 14

I. INTRODUCTION

Production of J/ψ (3100) and subsequent dilepton decay have been observed in hadron collisions by several experimental groups as well as dilepton production in the higher mass region. For instance, measurements of N (or $\overline{N}$)N → (μμ) + X have been performed by a Chicago-Illinois-Princeton group[1] at 225-GeV/c, a series of experiments by a Columbia-Fermilab-Stonybrook group[2] covering 2 < $M_{\mu\mu}$ < 10 GeV at 400 GeV/c, a Caltech - Stanford group[3] at 400 GeV/c and the NA-3 experiment[4] at the CERN-SPS covering 200- and 280-GeV/c beam momenta. They were under varying conditions of transverse momentum $p_\perp$ and Feynman x (x_F). We expect that a study of the spin dependence would be valuable in further specifying the character of the hadronic production mechanism.

In particular we propose to measure the single spin asymmetry, A_N, and the double spin asymmetry, A_{LL}, in the dimuon decays of J/ψ produced by polarized protons and antiprotons on a nuclear target and a polarized target. A first phase of operation with 400-GeV/c incident protons will allow measurements of A_N and A_{LL} with a 2% statistical accuracy. Asymmetries at 200 GeV/c for both p's and $\overline{p}$'s will be measured with a statistical accuracy of 5%.

II. PHYSICS JUSTIFICATION

A simple QCD model for J/ψ production[5] attracted our attention to the investigation of the spin dependence in J/ψ production.[6] It may be possible to measure the polarized gluon distribution functions in the nucleon if the

$pp \to (J/\psi) + X$ process is indeed dominated by gluon-gluon interactions such as claimed by many authors,[5-7] for instance,

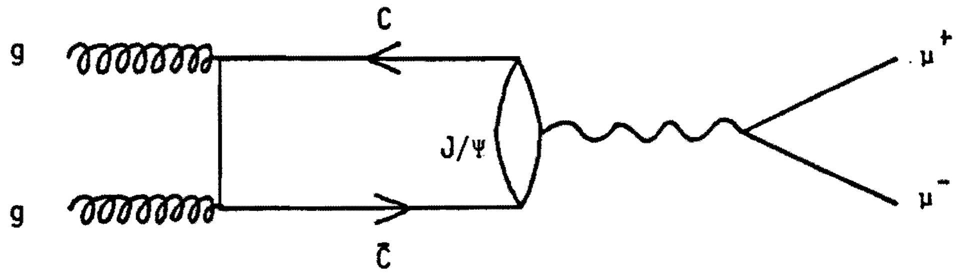

The entire diagram can be calculated simply. (This diagram involves three gqq vertices, the q being the heavy charmed quark. The coupling at each vertex is sufficiently weak for a perturbative calculation. The right-hand side of the diagram is experimentally known from e^+e^- collisions.) The measured one-spin and two-spin asymmetries (as defined below) of the $\mu^+\mu^-$ pair production thus give information on the initial gluon polarization, which can be used to reconstruct the gluon spin distribution in the polarized proton.

One spin measurement:

$$A_N = \frac{1}{P_B}\ \frac{d\sigma/dM(\uparrow) - d\sigma/dM(\downarrow)}{d\sigma/dM(\uparrow) + d\sigma/dM(\downarrow)} ,$$

two spin measurement:

$$A_{LL} = \frac{1}{P_B P_T}\ \frac{d\sigma/dM(\overset{\uparrow}{\downarrow}) - d\sigma/dM(\overset{\uparrow}{\uparrow})}{d\sigma/dM(\overset{\uparrow}{\downarrow}) + d\sigma/dM(\overset{\uparrow}{\uparrow})}$$

for a given x_F, where P_B is beam polarization, P_T is target polarization, and arrows indicate the spin direction in the laboratory system.

The first attempt to relate theoretically the initial gluon polarization to the parameter $A_{LL}(\vec{p}\vec{p} \to J/\psi + X)$ has been made.[6] We expect to see more work on this problem. We note here that we expect to observe a significantly large value of $\hat{A}_{LL}$ on the constituent level at small $p_\perp$ ($0 < p_\perp \ll M_{J/\psi}$) in J/ψ production.[7] If one only considers the above diagram, the allowed J_z would be 0, 1, and -1 at the intermediate state, where only q_c and $\overline{q_c}$ are involved. If the initial helicity state is (+-), that is ($\uparrow\downarrow$), then J_z = 2 and the process is forbidden; on the other hand for (++), that is ($\uparrow\uparrow$), then J_z = 0 and the process takes place. Therefore, the two-spin asymmetry on the constituent level becomes $\hat{A}_{LL} \cong + 100\%$, and the measured asymmetry $A_{LL} = (P_g)^2 \hat{A}_{LL}$, where P_g is the initial gluon polarization. So far, only one diagram has been discusssed, and the estimate of $\hat{A}_{LL}$ for other channels is not straightforward. From the SLAC quark spin-distribution data vs x_{BJ}, quarks are roughly 30% ($x_{BJ} \approx 0.15$) polarized for low -$p_\perp$ dimuon production in the central region. If we estimate that gluons are roughly aligned with the quarks then we expect $A_{LL} \cong + 10\%$, if $\hat{A}_{LL} = + 100\%$.

An attempt will be made to measure up to mass ≃ 4 GeV in $\vec{p}\vec{p} \to (\mu\mu) + X$, where the Drell-Yan process is significant, that is, valence quarks and sea quarks annihilate as:

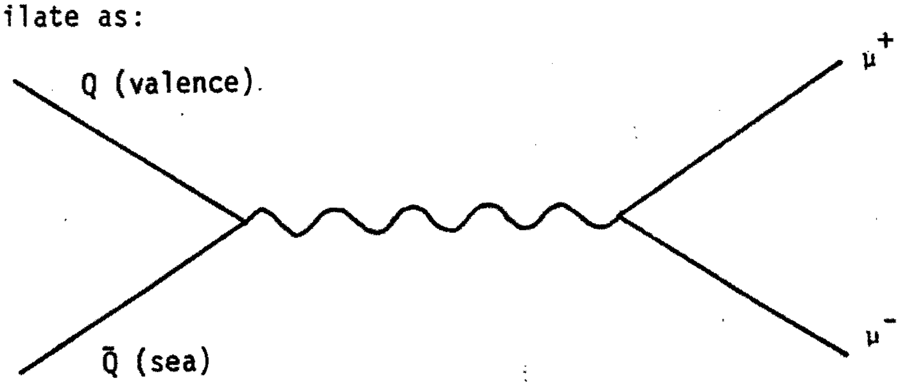

We note that the initial quark helicity states (++) are forbidden to produce the annihilation process because of helicity conservation resulting in $\hat{A}_{LL}$ = -100%. Thus, on the constituent level, $\hat{A}_{LL}$ switches from -100% to +100% and back to -100% in going thru the J/ψ region.

General bounds suggest that the one-spin asymmetry in proton-proton interactions could be 20 to 60%.[8]

We also propose to measure the parameter A_{LL} in $\vec{\bar{p}}\vec{p} \to \mu^+\mu^- X$ in the J/ψ region, which has the additional contribution of the direct-annhilation graph as:

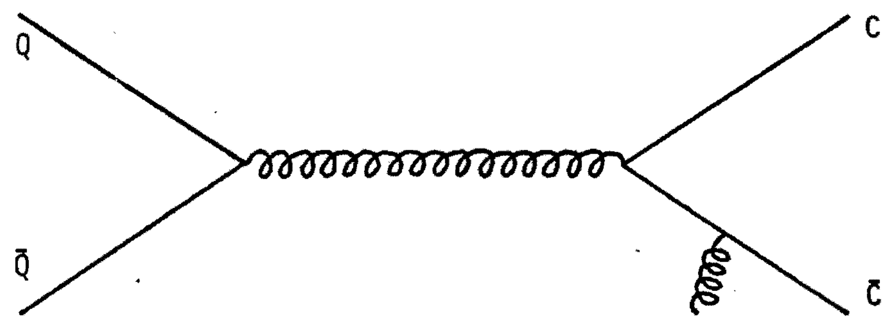

For this annihilation we expect $\hat{A}_{LL} \approx$ -100%. By comparing pp and $\bar{p}$p dilepton-production measurements, it may be possible to extract information on the $q\bar{q}$ annihilation mechanism. The spin-spin asymmetry in J/Ψ production would then give directly the product of the spin wave functions of the valence quarks in the proton and the valence antiquarks in the antiproton.

III. EXPERIMENTAL SETUP

Our main concern in the design of the apparatus is to obtain the largest acceptance for dimuons at the J/ψ mass region, because the cross section of this reaction is very small.

The dimuon mass can be obtained from the two muon's momenta p_1 and p_2 and their relative opening angle θ, as follows:

The dimuon mass can be obtained from the two muon's momenta p_1 and p_2 and their relative opening angle θ, as follows:

$$M^2_{\mu\mu} \cong 2\, p_1 p_2\, (1 - \cos\theta) \ .$$

The analyzing magnet is placed as close as possible (~ 3 m) to the polarized target. The magnet gives horizontal and vertical acceptance in the lab. of ± 12° and ± 4° respectively. The use of a commonly used hadron absorber placed right after the target is avoided in order to optimize the mass resolution and to avoid the problems of resolving events originating from the target and the hadron absorber.

A schematic view of the setup is shown in Fig. 1. The two muons in the final state are detected in a magnetic spectrometer consisting of the analyzing magnet, multi-wire proportional chambers (MWPC), drift chambers, a hadron filter, a magnetized iron, and scintillator hodoscopes.

Angles and momenta are determined with MWPC's (1-mm and 2-mm spacings), drift chambers, and the analyzing magnet (momentum kick = 0.4 GeV/c). Muon identification is done by the hadron filter, and magnetized iron is used to reject the low-momentum muons in order to obtain a reasonable trigger rate. Acceptance and mass resolution of this system are calculated by Monte Carlo simulation. The details of the calculation are described in Appendix I. Figure 2 shows the acceptance of the spectrometer with respect to x and dimuon mass. We expect that the acceptance for $J/\psi \to \mu\mu$ events is 35%, and the mass resolution is 2.5% at 400 GeV/c.

The wire chambers right downstream of the polarized target will see about 10^8 particles during the 20-msec spill. In the central region of P_3 and D_1, the rate will be less than ~ 150K/sec/wire and 350K/sec/wire respectively. The average multiple hit per wire for P_3 and D_1 will be less than 0.3 and 0.7 respectively. In the case of the drift chambers, drift space can be made shorter in the central region if necessary.

We note that in the case of poor spill structure the P3 chamber won't endure the rate, and we will be forced to use a hadron absorber between the polarized target and the SCM 105; in this case we have poorer mass resolution.

IV. POLARIZED BEAM

The polarized beam line in the meson lab will be used (E-581, construction of polarized beams). The characteristics of polarized beams are shown in Fig. 3.

Momentum bite:	$\Delta p/p = \pm 5\%$ (rms)
Angular divergence:	$\Delta\theta = 1$ mrad
Intensity:	$I = 3 \cdot 10^7$ protons/spill at 200 to 400 GeV/c,
	$3 \cdot 10^6$ antiprotons/spill at 200 GeV/c
Degree of polarization:	$P_B = 40$ to 50%
Beam size:	$\lesssim 2$ cm diameter

Beam MWPC's (P1 and P2) will define the beam position and angle to ± 0.3 mm and ± 0.1 mrad. It is important to monitor beam position stability because a systematic change in beam direction, correlated with spin reversal, can create a false asymmetry.

V. POLARIZED TARGET

The target will be either a polarized NH_3 or a ^{6}LiD target currently being developed at Saclay[9] (note that $^6\mathrm{Li} \approx \mathrm{D} + {}^4\mathrm{He}$). In fact both types of target may be useful in case the asymmetry effect from protons differs from neutrons. The target density for NH_3 or ^{6}LiD will both be 0.60 gm/cm^3, and the length will be 1/3 collision length. Assuming no shadowing effects, the polarization per nucleon will be 15% for NH_3 and 30% for ^{6}LiD.

VI. TRIGGER REQUIREMENT AND DATA COLLECTION

The trigger consists of two-muon detection and logic for a low-mass cut. The first part consists of a beam veto to eliminate muon halo, and at least 2 hits in each of T1, T2, T3 and T4 hodoscopes. A correlation in the vertical plane between horizontal slats of T2 and T3 can be used to constrain each muon to point approximately towards the polarized target region. To reduce the trigger rate, bending angles (vertical) in the magnetized iron are roughly measured by a correlation between T3 and T4 to reduce low-mass dimuons.

For the purpose of data collection all the hodoscope and MWPC information will be read into an on-line PDP-11 via CAMAC.

VII. EXPECTED BACKGROUND

There are a large number of muons coming from, for instance, decays of π's produced in the target. The result of Monte Carlo calculations indicate that the chance of forming false dilepton-coincidence events is indeed small although it depends on the mass region; estimates would be less than 10% of the J/ψ events. Low-mass accidentals are significantly large so that the magnetized iron located behind the hadron filter will be used to reject the trigger due to low-mass dilepton events. Probability of μ-decay in flight is $P_{\mu_i} = (1 - \exp(-L/\gamma_i c\tau)$, where $c\tau$ = 780 cm for π's and 371 cm for K's, and L is the distance from the PPT to Fe filter. At 400 GeV/c, the results of Monte Carlo calculations show that accidentals = 0.2 ev/spill while J/ψ = 2.4 ev/spill. The accidentals will increase with less mass and decrease with higher mass than the J/ψ mass as shown in Fig. 4. The noninteracting beam passes through a hole in the iron filter and through a deadened region of the MWPC's.

In case we require use of a hadron filter, an experimental setup is described in Appendix II. The advantage of this setup would be i) muon accidentals are negligible, and ii) the proportional or drift chambers will have no rate problems. Of course, this setup has serious disadvantages of poor mass resolution and poor vertex reconstruction.

VIII. RATES AND RUN PLAN

In order to obtain the statistical error of ± 0.02 to ± 0.05 covering the x_F region as shown in Fig. 2a, the running times required, assuming the use of the ^{6}LiD target, in the J/ψ mass region are:

	Beam Time	Statistical Accuracy
Phase 1 at 400 GeV/c	$p^{\uparrow}p \rightarrow (\mu\mu) + X \sim$ 100 hours	± 0.02
	$p^{\uparrow}p^{\uparrow} \rightarrow (\mu\mu) + X \sim$ 800 hours	± 0.02
at 200 GeV/c	$p^{\uparrow}p^{\uparrow} \rightarrow (\mu\mu) + X \sim$ 150 hours	± 0.05
Phase 2 at 200 GeV/c	$\bar{p}^{\uparrow}p \rightarrow (\mu\mu) + X \sim$ 150 hours	± 0.05
	$\bar{p}^{\uparrow}p^{\uparrow} \rightarrow (\mu\mu) + X \sim$ 700 hours	± 0.05

(cross section reference: Ref. 3)

IX. APPARATUS

1) Use a modified version of the existing Argonne polarized targets.
2) All the detectors including the beam polarimeter used in the beam diagnosis
3) Scintillation hodoscope, horizontal and vertical

   Vertical angular bin: ~ 5 mrad

Size of scintillators	Number of scintillators
T1 70 x 1.5 cm	40
T2 160 x 4 cm	40
T3 200 x 5 cm	40
T4 280 x 5 cm	64

4) Fast matrix coincidence logic

5) SCM-105 or equivalent

6) Multiwire proportional chambers (~ 3600 wires?)

Drift chambers (~ 850 cells)

Plane	Active Area(mm^2)	Wire Spacing (mm)	Number of wires
P1 X,Y	100 x 100	1.0	200
P2 X,Y	100 x 100	1.0	200
P3 X,Y,U	600 x 200	1.0, 1.5	1400
P4 X,Y,U	1600 x 400	2.0	1800
D1 X,Y,U	2000 x 600	20	190
D2 X,Y,U	3000 x 800	20	280
D3 X,Y,U	4000 x 1200	20	380

7) On-line computer to perform the following functions:

a) Control and measure target polarization

b) Record all the chamber and hodoscope events

c) Various on-line diagnostics

8) Fe filter

9) Magnetized iron

10) Hadron absorber, optional

References

1. K. J. Anderson et al., Phys. Rev. Lett. 42, 944 (1979), and references contained therein.

2. D. Hom et al., Phys. Rev. Lett. 37, 1374 (1976).

3. E. Siskind et al., Phys. Rev. D21, 628 (1980).

4. Proceedings of the Topical Conference of SLAC Summer Institute on Particle Physics, p. 434 (July, 1979); J. Badier et al., CERN/EP 80-150; CERN/EP 80-149; CERN/EP 80-36; Phys. Let. 86B, 98 (1979).

5. V. Barger, W. Y. Keuing, and R. J. N. Phillips, Phys. Lett. 91B, 253 (1980), and references contained therein; R. J. N. Phillips, Rapporteur talk at the XX International Conference on High-Energy Physics, Madison, Wisconsin, July, 1980.

6. K. Hidaka, to be published in the Proceedings of the International Symposium on High-Energy Physics With Polarized Beams and Targets, Lausanne, Switzerland, October, 1980.

7. Private communication with theorists at Argonne.

8. J. Soffer and P. Taxil, Nucl. Phys. B172, 106 (1980).

9. V. Bouffard, A. Abragam et al., to be published in Journal de Physique.

Figure Captions

Figure 1 Experimental setup.

Figure 2 a) Acceptance vs. x_F.

b) Acceptance vs. dimuon mass.

Figure 3 Expected intensity of polarized beam vs. momentum.

Figure 4 Accidental μ-pair vs. mass.

Figure 5 An experimental setup using a hadron absorber.

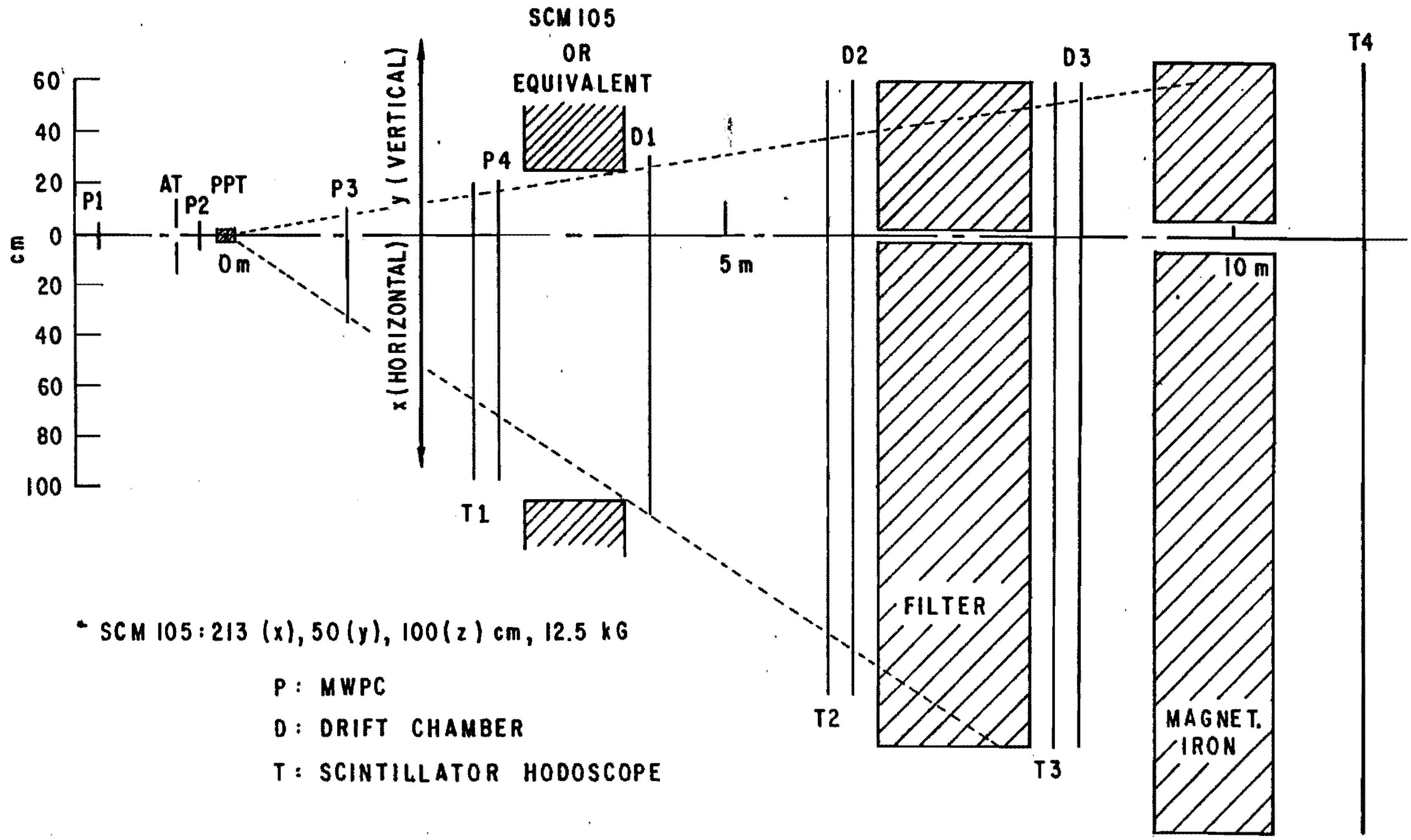
SCM 105
OR
EQUIVALENT
D2
D3
T4
60
40
20
0
20
40
60
80
100
cm
P1
AT
P2
PPT
0 m
P3
y (VERTICAL)
x (HORIZONTAL)
P4
D1
5 m
10 m
T1
T2
T3
FILTER
MAGNET.
IRON
* SCM 105: 213 (x), 50 (y), 100 (z) cm, 12.5 kG
P: MWPC
D: DRIFT CHAMBER
T: SCINTILLATOR HODOSCOPE

Figure 1

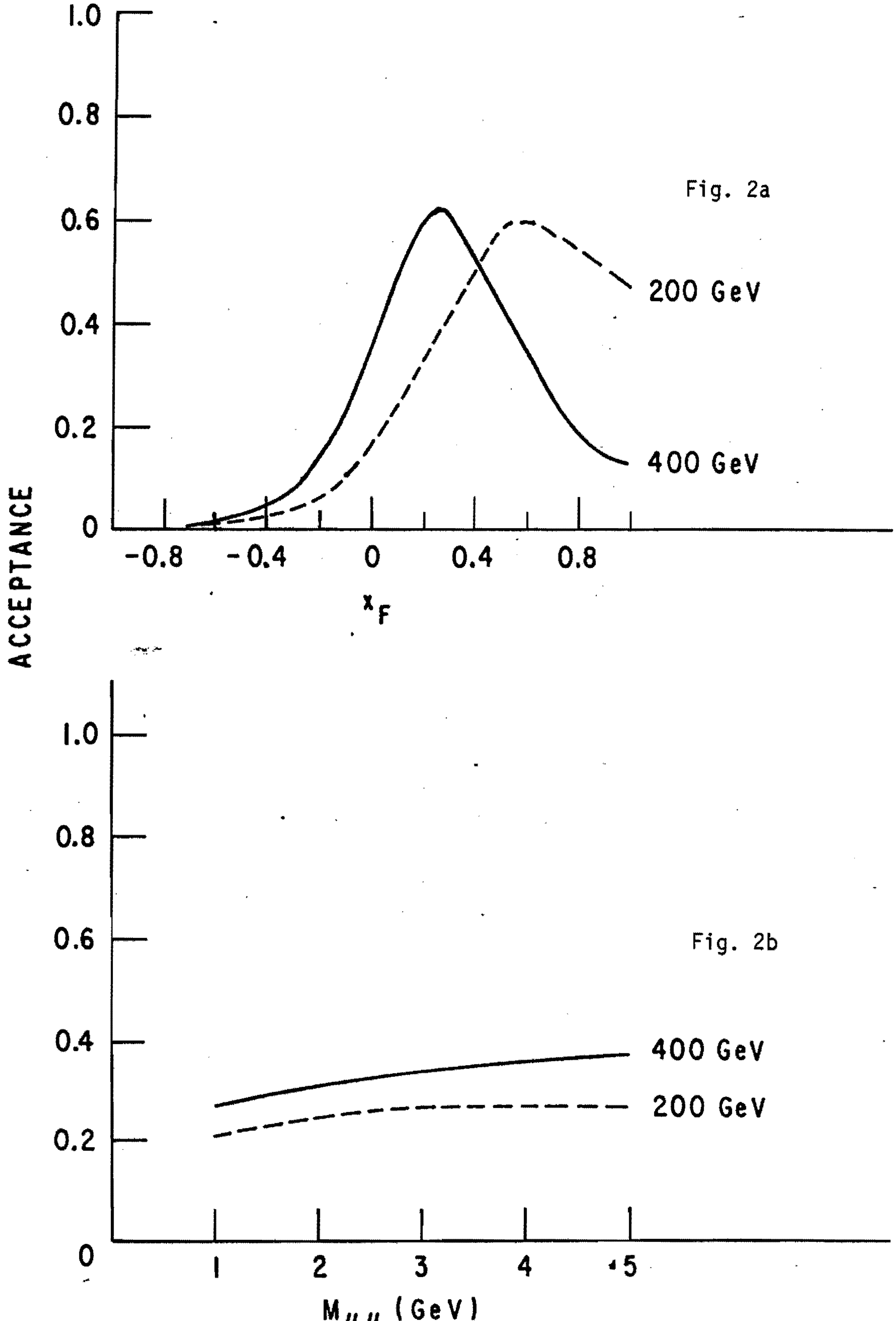
1.0
0.8
0.6
0.4
0.2
0
ACCEPTANCE
200 GeV
400 GeV
−0.8
−0.4
0
0.4
0.8
x_F
1.0
0.8
0.6
0.4
0.2
0
400 GeV
200 GeV
1
2
3
4
5
$M_{\mu\mu}$ (GeV)

Fig. 2a

Fig. 2b

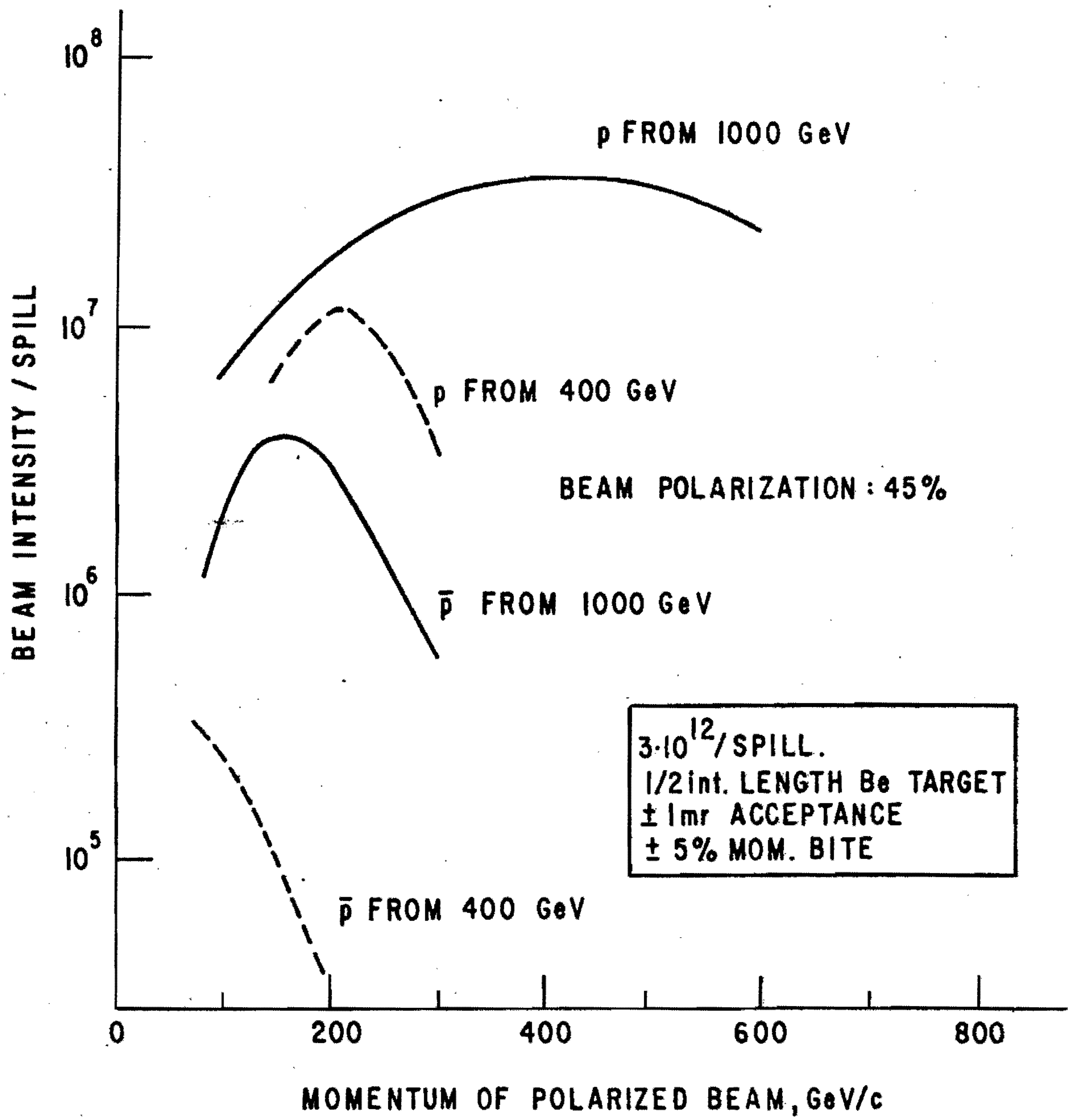

p FROM 1000 GeV
p FROM 400 GeV
BEAM POLARIZATION : 45%
$\bar{p}$ FROM 1000 GeV
3·10^12/SPILL.
1/2 int. LENGTH Be TARGET
± 1mr ACCEPTANCE
± 5% MOM. BITE
$\bar{p}$ FROM 400 GeV
BEAM INTENSITY / SPILL
10^8
10^7
10^6
10^5
0
200
400
600
800
MOMENTUM OF POLARIZED BEAM, GeV/c

Figure 3

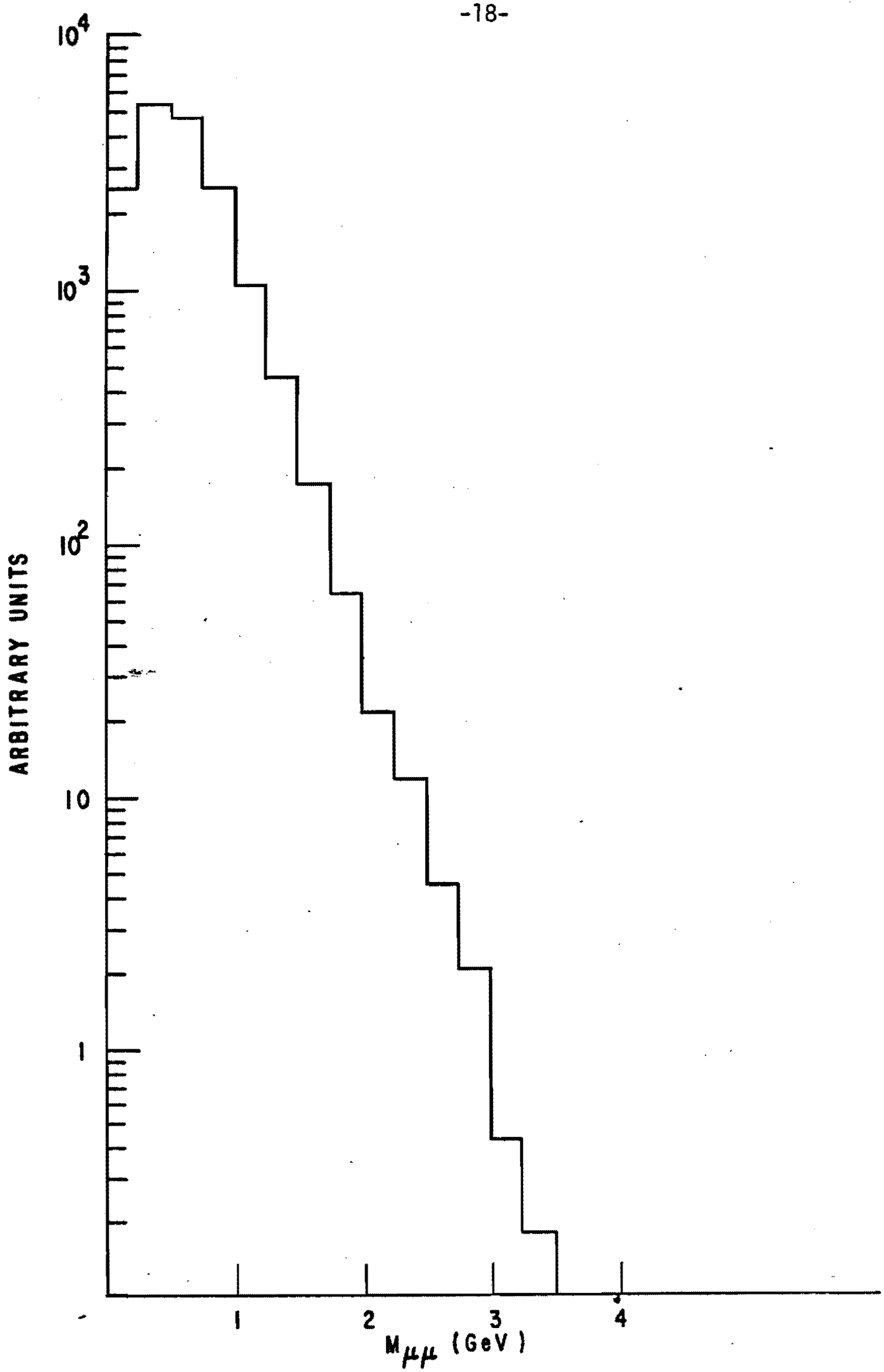

Figure 4

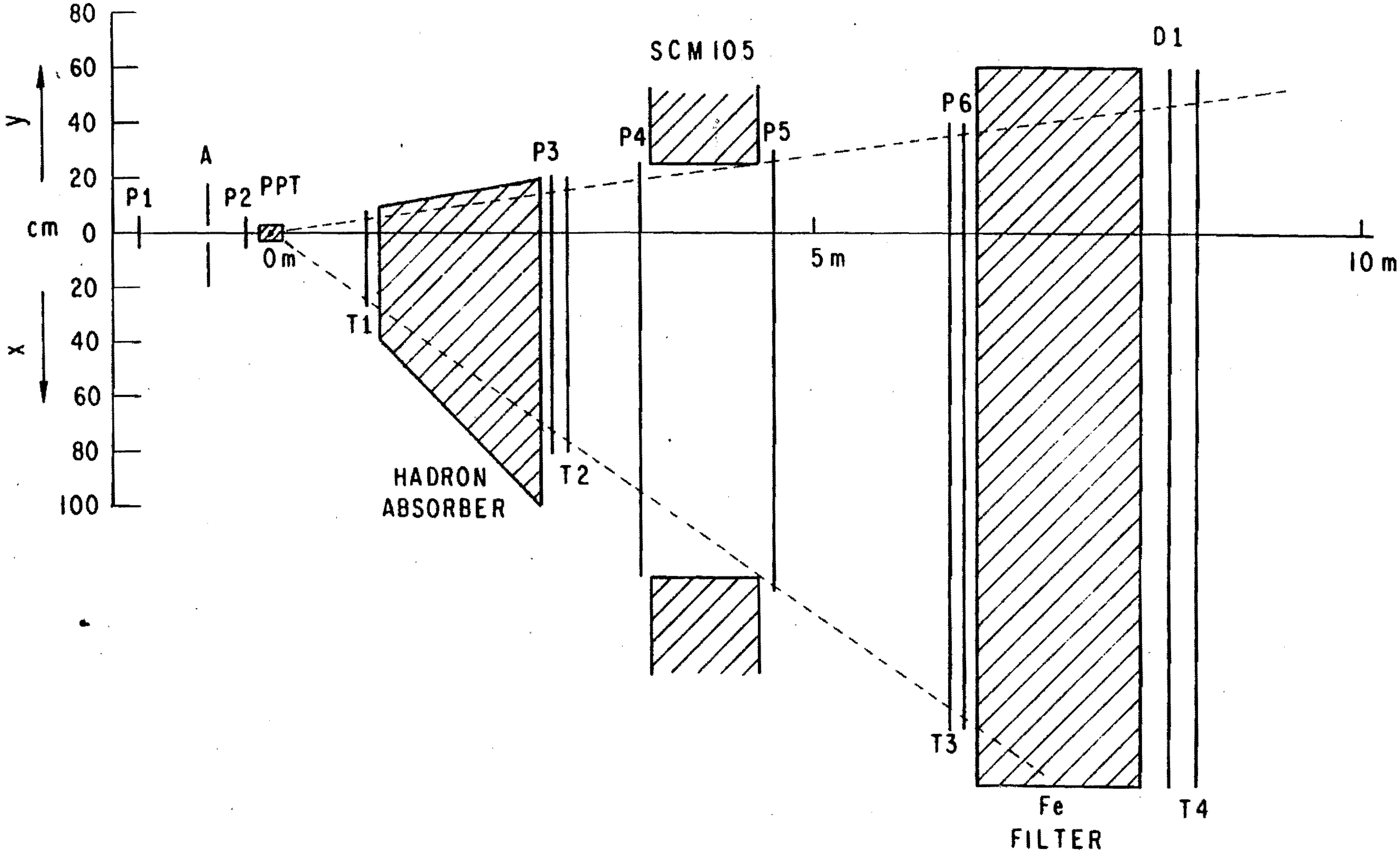
80
60
40
20
cm 0
20
40
60
80
100
y
x
P1
A
P2
PPT
0 m
T1
HADRON
ABSORBER
P3
T2
P4
SCM 105
P5
5 m
P6
T3
Fe
FILTER
D1
T4
10 m

Figure 5

APPENDIX I

In the Monte Carlo calculation the following invariant cross section in terms of x_F and $p_\perp$ distributions of J/ψ production was used (Ref. 1).

$$E \frac{d^3\sigma}{dp^3} \approx \exp(-2p_\perp)(1-x_F)^{3.44} \ .$$

Slightly different formulae obtained elsewhere[2-4] are also used but the results are almost unchanged. Decay angle distribution is assumed to be constant in the calculations. (Note that in polarization experiment we can measure the differnt spin observables by measuring decay angle distribution.)

The overall efficiency for the $J/\psi \to \mu\mu$ events for the setup shown in Fig. 1 is 0.36 with a small-angle cut (a small hole in the iron filter) as shown in Fig. 1 at 400 GeV/c, and is 0.26 at 200 GeV/c.

The Mass Resolution

The mass resolution, $\delta M/M$ (sigma), is estimated as follows:

$$\left(\frac{\delta M}{M}\right)^2 = \tfrac{1}{4}\left(\frac{\delta p_1}{p_1}\right)^2 + \tfrac{1}{4}\left(\frac{\delta p_2}{p_2}\right)^2 + \frac{(\delta\theta_1)^2 + (\delta\theta_2)^2}{(\theta_1 + \theta_2)^2} ,$$

where p and θ represents momentum and angle of one of the muon pair.

i) $\delta M/M \approx$ 2 to 3% when chamber P3 is utilized.

ii) $\delta M/M \approx$ 8% without chamber P3, but $\pm$ 10 mrad cut (the use of steel-filter magnets may be helpful to improve the resolution).

APPENDIX II

An experimental setup using a hadron absorber is shown in Fig. 5. The overall efficiency for the J/ψ production is somewhat lower than the case of Fig. 1 as discussed below, but mass resolution is worsened.

Obviously for events at small angles we are unable to reconstruct a good vertex and thus distinguish events from the polarized target and the hadron absorber. We estimate the multiple scattering in the absorber to be:

$$\theta_{rms} = \frac{0.014}{p} \sqrt{L/R} \left(1 + \frac{1}{9} \log \frac{L}{R}\right),$$

if L = 150 cm, p = 20 GeV, then $\theta_{rms} \approx 8$ mrads.

Monte Carlo shows that useful events will be limited to those with an angle > 20 mrads for clear target-absorber vertex separation. The Monte Carlo simulation also shows the mass resolution will be ~ 8% below J/ψ mass region.